IDŐJÁRÁS

Quarterly Journal of the Hungarian Meteorological Service
Vol. 118, No. 1, January – March, 2014, pp. 53–77

Sensitivity analysis of microscale obstacle resolving models for an idealized Central European city center, Michel-Stadt

Anikó Rákai[1*], **Gergely Kristóf**[1], and **Jörg Franke**[2,3]

[1]*Department of Fluid Dynamics, Budapest University of Technology and Economics, Bertalan L. u. 4-6, H-1111 Budapest, Hungary*
E-mails: rakai@ara.bme.hu, kristof@ara.bme.hu

[2]*University of Siegen, Institute of Fluid- and Thermodynamics, 56068 Siegen, Germany*

[3]*Vietnamese-German University (VGU), Binh Duong New City, Vietnam, joerg.franke@vgu.edu.vn*

**Corresponding author*

(Manuscript received in final form March 8, 2013)

Abstract—Microscale meteorological models with obstacle resolving grids are an important part of air quality and emergency response models in urban areas providing the flow field for the dispersion model. The buildings as bluff bodies are challenging from the discretization point of view and have an effect on the quality of the results. In engineering communities the same topic has emerged, called computational wind engineering (CWE), using the methods of computational fluid dynamics (CFD) calculating wind load on buildings, wind comfort in the urban canopy, and pollutant dispersion. The goal of this paper is to investigate the sensitivity of this method to the discretization procedure used to resolve the urban canopy with meshes which are of operational size, i.e., which can be run on a single powerful computer of a design office as well. To assess the quality of the results, the computed mean and rms (root mean square) velocity components are compared to detailed wind tunnel results of an idealized Central European city center, Michel-Stadt. A numerical experiment is carried out where the numerical sensitivity of the solution is tested by additional solutions on different grid resolutions (at least 3 stages of grid refinement), unrelated grid types (tetrahedral, polyhedral, Cartesian hexahedral, and body fitted hexahedral, all automatically generated), and different discretization schemes. For an objective qualitative judgment two metrics are investigated, the well know hit rate and another metric that does not depend on threshold values. The quality of the meshes is investigated with correspondence to the numerical stability, CPU-time need, and grid quality metric. It is shown that the solution with the best resulting metric is not necessarily the most suitable for operational purposes and almost 20% difference in the hit rate metric can result from different discretization approaches.

Key-words: microscale air quality models, obstacle resolving, urban flow, polyhedral mesh, snappyHexMesh, OpenFOAM®

1. Introduction

Prognostic microscale obstacle resolving meteorological models and computational wind engineering (CWE) models deal with the common fields of wind and pollutant dispersion modeling inside the urban canopy. *Baklanov* and *Nuterman* (2009) show that these models with increasing computational capacity can be the final scale in a nested multi-scale meteorological and dispersion model. *Mészáros et al.* (2010) have also shown a coupled transport and numerical weather prediction system for accidental pollutant releases. They say that a microscale resolved model is also needed and investigated resolving obstacles at the smallest scale with a computational fluid dynamics (CFD) model in *Leelőssy et al.* (2012).

Stull (1988) defines microscale in meteorology being a few kilometers or less where the typical phenomena include mechanical turbulence caused by the buildings. *Britter* and *Hanna* (2003) suggest the following length-scales: regional (up to 100 or 200 km), city scale (up to 10 or 20 km), neighborhood scale (up to 1 or 2 km), and street scale (less than 100 to 200 m). The two last correspond to the microscale definition of *Stull* and are used in this paper.

Baklanov (2000) showed the possibilities and weaknesses of using CFD for air quality modeling and concluded that they have a good potential. *Balczó et al.* (2011) showed a real life test case of dispersion studies of motorway planning around Budapest, carried out with the code MISKAM®, compared to wind tunnel measurements. That was an extensive example of using microscale meteorological and dispersion models for operational purposes and also showed its difficulties. To be able to use these models with confidence for operational purposes in air quality forecasting or emergency response tools, without using additional experiments, a detailed knowledge on their quality is necessary.

There are several research groups dealing with this field who have issued best practice guidelines, mainly based on validation studies compared with wind tunnel measurements of fairly simple cases. Wind tunnel models are used because of the well defined boundary conditions and the relative ease of high resolution measurement points compared to full scale field models. In these microscale validation studies usually steady state flow models are used, assuming neutral stability and neglecting the Coriolis forces. The two most thorough guidelines are from the Architectural Institute of Japan (*Tominaga et al.*, 2008), and from a COST project, Quality assurance of microscale meteorological models (*Franke et al.*, 2011). The German Engineering Community has also a standard on validation of microscale meteorological models for urban flows with a database of simple building configurations (*VDI*, 2005).

Several studies have dealt with the problem of defining inflow conditions for the atmospheric boundary layer, the most influential being *Richards* and *Hoxey* (1993). There was a considerable effort on defining inflow conditions which are maintained throughout the computational domain if no buildings are inside, i.e., aiming for lateral homogeneity, see *Blocken et al.* (2007a), *Yang et al.* (2007), *Parente et al.* (2010), *O'Sullivan et al.* (2011), and *Balogh et al.* (2012).

Another huge effort was made for developing turbulence models which are the best for the purpose of Computational Wind Engineering. Since buildings are bluff bodies, the stagnation point anomaly revealed by *Durbin* (1996) gives a challenge for the turbulence models. There were attempts to improve the linear approach of the Boussinesq assumption and choose the best model; a wide comparison of the possibilities is shown in *Tominaga et al.* (2004) and *Yoshie et al.* (2005). Nonlinear turbulence models were also considered for flow around a single cube obstacle by *Erhard et al.* (2000) and *Wright* and *Eason* (2003), and for topographical features by *Lun et al.* (2003).

The numerical discretization procedure has less focus but it can also have a significant effect on the quality of computations. In engineering communities, dealing with computational fluid dynamics (CFD), quality assurance, verification and validation, and numerical uncertainty analysis are becoming more and more important; see e.g., *Roache* (1997) , *Oberkampf* and *Trucano* (2002), and *Franke* (2010).

This paper shows different numerical discretization possibilities for a test case called Michel-Stadt. This is an idealized Central European city center investigated in a wind tunnel with detailed measurement results publicly available. When meshing a complex urban geometry, several approaches are possible, with different quality in performance and results, and with different cost in the meshing and computing procedure. *Franke et al.* (2012a) and *Hefny* and *Ooka* (2009) are the only ones to the knowledge of the authors who compared different mesh types when investigating microscale meteorological or air quality models. *Franke et al.* (2012a) compared a block-structured hexahedral meshing approach to an unstructured hexahedral and an unstructured hybrid mesh which consists of tetrahedral and prism elements, the latter comprising of 3 layers around the geometries. They investigated simple block geometries and rows of blocks, thus simpler urban arrangements than the one presented in this paper. Their findings about the quality of the results of mean velocity components compared to experiments showed that the unstructured meshes yield often better metrics which they attributed to the higher resolution of those meshes. In this paper different resolution is used for each mesh to enable to compare similar resolutions. For the geometry of rows of blocks, *Franke et al.* (2012a) found that second order simulations with unstructured meshes are unstable, which is similar to the findings of this paper. *Hefny* and *Ooka* (2009) compared hexahedral and tetrahedral elements only for a simple block geometry, and they compared the results of dispersion to each other. In their findings the hexahedral mesh had the best performance regarding estimated numerical error, but they did not compare the results to experimental values. There is no comparison for the flow field in their paper either, which determines the results of the dispersion essentially. The study presented here gives important additional information to these two papers in several points. The geometry used is more complex, information about the computational cost is given qualitatively for the mean and turbulent velocity components as well (dispersion studies will be carried out in the next stage of the research), and the stability of the numerical solution is also addressed in a systematic way. Apart from the hexahedral and tetrahedral meshes, here a polyhedral mesh type is also used.

In the present paper, four mesh types are compared from the points of view mentioned above, a tetrahedral, a polyhedral, a Cartesian hexahedral, and a body fitted hexahedral mesh. At least 3 spatial resolutions and 3 discretization approaches of the convective term are considered for each mesh. For the calculations the open source CFD code, OpenFOAM® was used. It was already validated by *Franke et al.* (2012a) for simple obstacle geometries and by *Rakai* and *Kristof* (2010) for the Mock Urban Setting Test used in the COST Action 732. The test-case used in this study was also already calculated and compared to results of ANSYS® Fluent by *Rakai* and *Franke* (2012), which is a widely used industrial CFD code for CWE, and the results were similar with the two different codes.

The goal of the paper is to show the change in computational cost and quality of the results via statistical metrics of the mean and rms (root mean square) velocity components measured inside the urban canopy.

In Section 2, the numerical experiment is described with a detailed description of the case study, the numerical discretization methods, and the metrics used for comparison. In Section 3, results are shown from different viewpoints and conclusions are drawn in Section 4 with an outlook to future work.

2. *Numerical experiment*

2.1. Case study

The chosen case study is an idealized Central European city centre, Michel-Stadt. It was chosen as it is a complex geometry with detailed measurement results available (*Fischer et al.*, 2010). In the COST Action 732 (*Schatzmann et al.*, 2009) on the Quality assurance of microscale meteorological models, a more simple (Mock Urban Setting Test, simple rows of identical obstacles) and a more complex (a part of Oklahoma city) test-case was used, and it was found that an in-between complexity would be beneficial. In the COST Action ES 1006 on the Evaluation, improvement and guidance for the use of local-scale emergency prediction and response tools for airborne hazards in built environments (http://www.elizas.eu/), the Michel-Stadt case is used for the first evaluations.

Two component LDV (laser doppler velocimeter) measurements were carried out in the Environmental Wind Tunnel Laboratory of the University of Hamburg. They are part of the CEDVAL-LES database (http://www.mi.uni-hamburg.de/Data-Sets.6339.0.html), which consists of different complexity datasets for validation purposes. This case, Michel-Stadt, is the most complex case of the dataset. There are two versions of it, one with flat roofs and another with slanted roofs. In this paper the flat-roof case is used. 2158 measurement points are available for the flow field; they can be seen in *Fig. 1*. They consist of 40 vertical profiles (10–18 points depending on location for each), 2 horizontal planes (height 27 m and 30 m, 225 measurement points for each), and 3 so-called street canyon planes (height 2 m, 9 m and 1 m, 383 measurement points for each), which are located inside the urban canopy.

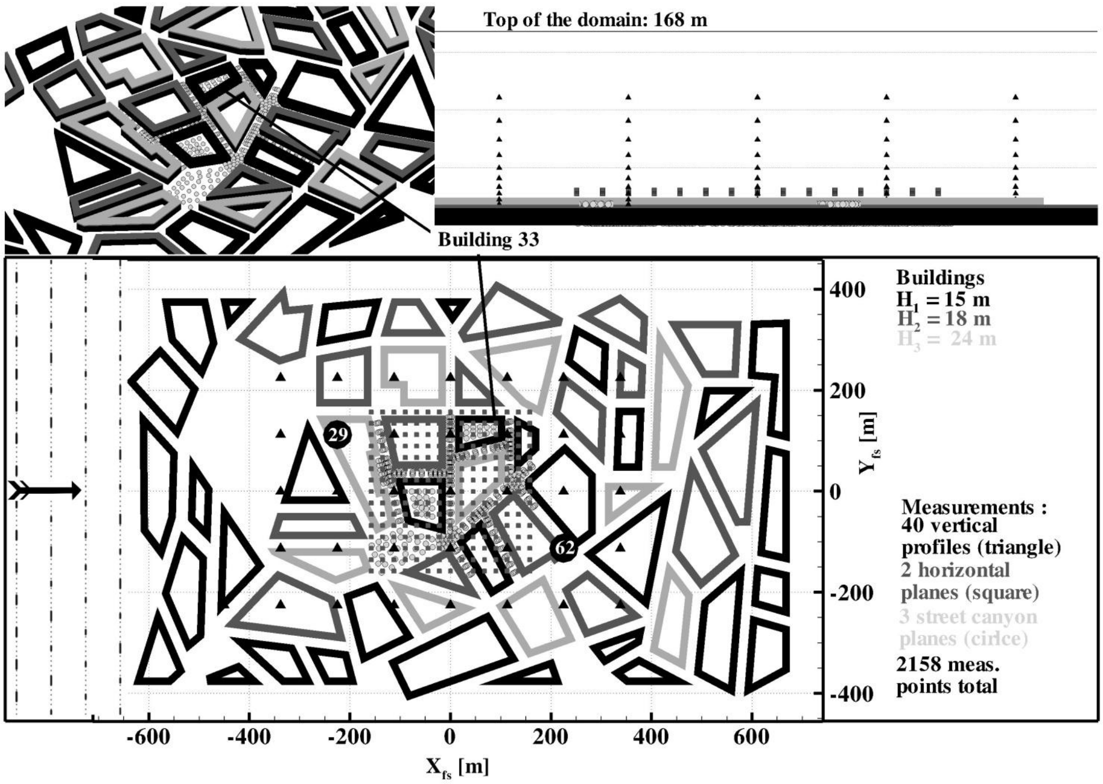

Fig. 1. Michel-Stadt with measurement points, Building 33 highlighted, the location of the roughness elements is just illustration, not exact.

The two available components are the streamwise and lateral velocity components, and time series are available for each of them. The dataset also contains the statistically evaluated mean (U_{mean}-streamwise, V_{mean}-lateral), rms (U_{rms}-streamwise, V_{rms}-lateral), and correlation values for comparison with steady state computations.

Approach flow data are provided from 3 component velocity measurements. The approach flow is modeled as an atmospheric boundary layer in the wind tunnel with the help of spires and roughness elements.

2.2. Computational model and boundary conditions

The computational domain was defined to correspond with the COST 732 Best Practice Guideline (*Franke et al.*, 2007) (*Fig. 1*), which resulted in a 1575 m × 900 m × 168 m domain, with a distance of the buildings of 11 H_3 from the inflow, 9.4 H_3 from the outflow, and at least 6 H_3 from the top boundaries, where $H_3 = 24$ m is the highest building's height. The computations were done in full scale, while the experiment was done at a scale of 1 : 225. The dependence of the results on this scale change was investigated by *Franke et al.* (2012b) using both full scale and wind tunnel scale simulations, and only a small difference in the statistical validation metrics was observed.

As *Roache* (1997) explains, the governing partial differential equations (PDE) and their numerical solution both add up to the total error of the simulation. To have a better view of the effect of the numerical discretization (and the resulting numerical error), the governing PDEs were kept the same during all the numerical experiments.

As inflow boundary condition, a power law profile (exponent 0.27, with a reference velocity $U_{ref} = 6.11$ m/s defined at $z_{ref} = 100$ m) fitted to the measured velocity values was given. This corresponds to a surface roughness length $z_0 = 1.53$ m. *Britter* and *Hanna* (2003) define this as a very rough or skimming approach flow. The turbulent kinetic energy and its dissipation profiles were calculated from the measured approach flow values by their definition and equilibrium assumption. At the top of the domain the measurement values corresponding to that height were fixed. The lateral boundaries were treated as smooth solid walls, as the computational domain's extension is the same as the wind tunnel width. The floor, roughness elements, and buildings were also defined as smooth walls. Standard wall functions were used. As the roughness elements are included in the domain, there is no need to use rough wall functions for the approach flow, and also the problem of maintaining a horizontally homogeneous ABL (atmospheric boundary layer) profile, which is reported (*Blocken et al.*, 2007b) to be problematic for this kind of modeling, is avoided. *Franke et al.* (2012b) have shown in a further investigation that this is not necessary as the flow is governed by interacting with the first buildings. They compared the modeling of the roughness elements explicitly and implicitly and found little influence on the results.

The Reynolds Averaged Navier-Stokes Equations were solved with standard k-ε turbulence model and the SIMPLE (semi-implicit method for pressure linked equations) method was used for pressure-velocity coupling (*Jasak*, 1996).

2.3. Discretization of the governing PDFs

As was stated before, numerical discretization has an effect on the results of the solution due to numerical error. In complex geometries its exact quantification is difficult as no analytical solution of the governing equations exists, but with a numerical experiment the effect can be investigated. In the following the mesh type, spatial resolution and the convective term discretization used for Michel-Stadt is explained. All the meshes were generated automatically which is a necessity for using this model for operational purposes and general building configurations.

2.3.1. Spatial discretization

Four mesh types are compared; their visual appearance is illustrated always for Building 33, highlighted in *Fig. 1*:

- *Unstructured full tetrahedral Delauney mesh generated with ANSYS® Icem.*

For the creation of the Delauney volume cells, first an Octree mesh was created and kept only at the surfaces, the Delauney mesh was grown from that surface mesh (*Fig. 2a*). The coarsening of the meshes was carried out by scaling the defined minimum length scales in ANSYS® Icem by 1.6. Resolution of buildings was given by the minimum face and edge size on each building. The maximum allowed expansion ratio was given for the Delauney algorithm.

- *Unstructured full polyhedral mesh created by ANSYS® Fluent from the tetra mesh.*

The polyhedral meshes were converted from the original tetrahedral meshes by ANSYS® Fluent. Each non-hexahedral cell is decomposed into sub-volumes called duals which are then collected around the nodes they belong to in order to form a polyhedral cell (see *Ansys*, (2009) for more details). The refinement ratio is thus kept very similar to the one in case of the tetra meshes(*Fig. 2b*).

- *Cartesian hexahedral mesh created with snappyHexMesh of OpenFOAM®.*

As the main research tool for these investigations is OpenFOAM®, its open source meshing tool is also used for mesh generation. This is done first by creating a Cartesian castellated mesh by refining around a given file in STL format and deleting cells inside the geometry. This mesh was also investigated in the studies (Fig. 2c), as the generation process for this one in much faster than for any of the other meshes mentioned. Building resolution cannot be given explicitly, only the resolution of the starting domain and the number of refinement iteration cycles can be defined.

- *Body fitted hybrid mesh with mostly hexahedral elements meshed with snappyHexMesh of OpenFOAM®.*

The Cartesian mesh is snapped to the edges of the geometry (*Fig. 2d*) as a next step, which takes approximately 10 times more time as the creation of the Cartesian mesh.

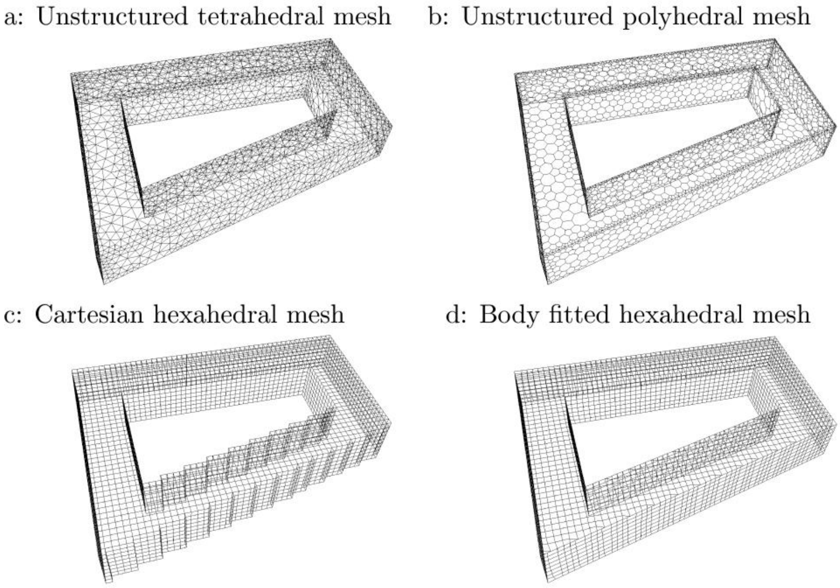

Fig. 2. Coarsest surface meshes on Building 33.

The grid convergence performance of the meshes was also investigated; at least 3 different resolutions were used for each mesh type. This makes it possible to use them for numerical uncertainty estimation at a later stage of the study.

The cell numbers of the investigated meshes can be found in *Table 1*. To have a better idea of the resolution of urban area and the buildings, in *Table 2* the number of faces on Building 33 is shown. This building was chosen as it is in the measured area close to other buildings, thus it is an indicator of street canyon resolution. The entire surface area of this building is approximately 12 000 m^2.

As it can be seen, the resolution on the building for different mesh types is not in linear relation with the total cell numbers of that mesh. See, e.g., in *Table 1* that the coarsest polyhedral mesh has 1.7 million cells and 4038 faces on the building, while the coarsest tetrahedral mesh has 6.65 million cells and 4317 faces on the building.

Table 1. Cell numbers (million cells) of the investigated meshes

	coarsest				finest
polyhedral	1.73	–	3.21	–	6.17
tetrahedral	6.65	–	13.17	–	26.79
Cartesian hexahedral	2.39	3.97	8.04	14.23	27.52
body fitted hexahedral	2.40	3.97	8.04	14.23	27.52

Table 2. Face numbers on Building 33

	coarsest				finest
polyhedral	4038	–	7455	–	12293
tetrahedral	4317	–	8934	–	15987
Cartesian hexahedral	3600	5486	11780	19879	36525
body fitted hexahedral	3416	5217	11180	18854	34660

2.3.2. Mesh quality

If we would like to resolve complex geometries properly, a compromise in mesh quality is unavoidable. This can cause a decrease both in numerical accuracy and stability of the computations, for more detail see *Jasak* (1996).

Some general measures on mesh quality to keep in mind when creating a mesh are the following:

- *Cell aspect ratio*

  Ratio of longest to shortest edge length is best to keep close to 1.

- *Expansion ratio/cell volume change*

  Ratio of the size of two neighboring cells is best to keep under 1.3 in regions of high gradients (*Franke et al.*, 2007).

- *Non-orthogonality*

  Angle α between the face normal $\underline{S}$ and PN vector connecting cell centers P and N is best to keep as low as possible, see in *Fig. 3.*

- *Skewness*

  Distance between face centroid and face integration point is best to keep as low as possible, see $\underline{m}$ in *Fig. 3*. In OpenFOAM® this value is normalized by the magnitude of the face area vector $\underline{S}$.

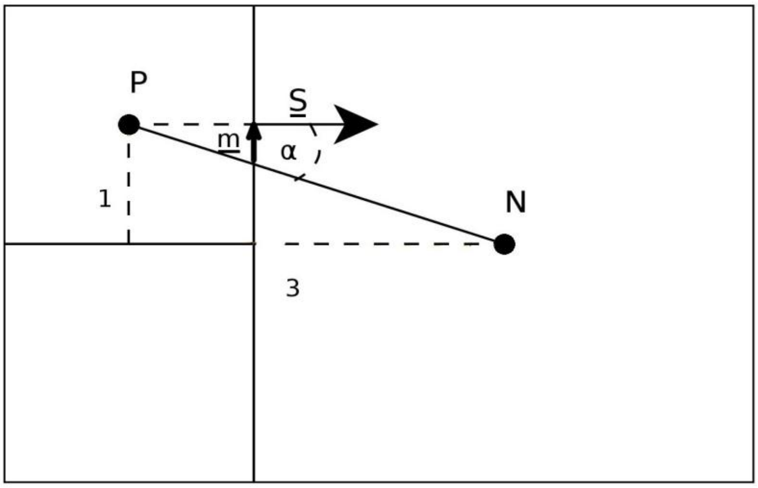

Fig. 3. Non-orthogonality and skewness.

2.3.3. Discretization of the convective/advective term

The discretization of the convective/advective terms of the transport equations solved is an important source of numerical discretization error. Upwind schemes use the values of the upwind cell as face value for the flux calculation (*Jasak*, 1996).

Central differencing uses a linear interpolation of the upwind and downwind cell value for the face value, which is of higher accuracy but may be unstable. Other schemes are defined as combination of the two for an optimal compromise between accuracy and stability (*Jasak*, 1996), like linearUpwind (a first/second order, bounded scheme) in OpenFOAM® (*OpenCFD Limited*, 2011) or second order upwind in ANSYS® Fluent (*Ansys*, 2009).

Different schemes can be used for the different variables, and to reach convergence, the following was found to be useful in OpenFOAM®:

- Initialize the solution domain with a potential flow solution.
- Use full upwind schemes for all convective terms.
- Use linearUpwind for momentum equation convective terms, upwind for the turbulence equations.
- Use linearUpwind for all convective terms.

The discretization of the pressure equation used to enforce mass conservation and all other gradients was approximated with the linear Gauss scheme. This can also add up to the instability of the solution.

It is important to note here that using higher order schemes of the convective/advective terms for meteorological models is not straightforward. E.g., in the MISKAM® model, which is a microscale operational model for urban air pollution dispersion problems, only upwind-differences are used for the discretization of the advection terms in the momentum equations (*Eichhorn*, 2008). *Janssen et al.* (2012) also shows that for certain meshes the use of higher order terms can cause convergence problems, so users may be forced to use lower order discretization. They suggest a not automatically generated hexahedral mesh to avoid this problem.

2.4. Validation metrics

With all the modeling and numerical errors inherent in the simulations, it is of vital importance to compare the simulation results to measurements. This way one can gain more information on the performance of the model. In case of wind engineering, the simulations are usually compared to wind-tunnel experiments as they are more controllable than field experiments with regard to boundary/meteorological conditions and have smaller measurement uncertainties, see *Schatzmann* and *Leitl* (2011) and *Franke et al.* (2007).

The most straightforward and inevitable part of the comparison is visual comparison with the aid of vertical profiles, contour and streamline plots, scatter plots, etc. It is also important, however, to quantify the differences in the models, for which reason validation metrics are used.

- *HR*

The most widespread metric in CWE (see, e.g., *VDI* (2005), *Schatzmann et al.* (2009), and *Parente et al.* (2010)) for wind velocity data is hit rate, which can be defined as in Eq. (1), where S_i is the prediction of the simulation at measurement point i, E_i is the observed experimental value, and W is an allowed absolute deviation, based on experimental uncertainty. N is the total number of measurement locations.

$$HR = \frac{1}{N}\sum_{i=1}^{N} \delta_i \, ,$$

$$\delta_i \begin{cases} 1 for \left|\frac{S_i - E_i}{E_i}\right| \leq 0.25 \vee |S_i - E_i| \leq W \\ 0 for else \end{cases} . \tag{1}$$

The allowed relative deviation in Eq. (1) was used as 25% first in the VDI guideline (*VDI*, 2005), and from thereon this value is used by the CWE community. A disadvantage of the hit rate metric is that it takes into consideration only the experimental uncertainty and it is sensitive to the used allowed experimental uncertainty (*W*) value. More detail on this can be found in the Background and Justification Document of the COST ES1006 Action (*COST ES1006*, 2012). When comparing different simulations with the same allowed threshold values, differences can equally be seen.

For the investigated Michel-Stadt case, the allowed absolute uncertainty was defined by *Efthimiou et al.* (2011) only for the streamwise and lateral normalized velocity components (0.033 for U_{mean} / U_{ref} and 0.0576 for V_{mean} / U_{ref}), so the calculation of the metric would only be possible for those variables. However, as time dependent measurement series are available and statistical results are also provided by the *EWTL*, it is beneficial to compare also the Reynolds stress components. Here the normalized diagonal components are shown as they are used to calculate turbulent kinetic energy, which will be of vital importance for the dispersion simulations.

For the allowed absolute uncertainty in the hit rate metric, different values were tested. It was found that the relation of metrics to each other is independent of the chosen value, so 0.003 are used for both U_{rms} / U_{ref} and V_{rms} / U_{ref}, which were found to be appropriate to have sensible values between 0 and 1 for the hit rate metric.

- *L2 norm*

Using matrix norms for comparison is also possible. With *L2* norm, the negative values of velocity components are not problematic. This metric can be seen as a normalized relative error of the whole investigated dataset.

$$L2 = \frac{\sqrt{\sum_{i=1}^{N}(E_i - S_i)^2}}{\sqrt{\sum_{i=1}^{N} E_i^2}}. \tag{2}$$

Finally, it is important to note that the most recent papers dealing with numerical uncertainty suggest metrics incorporating both experimental and numerical uncertainties in validation metrics as validation uncertainty, see, e.g., *Eca* and *Hoekstra* (2008). It is an important part of the quality assurance process and will be regarded in a separate publication.

3. Results and discussion

3.1. Mesh quality evaluation

The grid quality measures explained in Section 2 are investigated first for the mesh types used for the computations. The values of the quality metrics are shown in *Fig. 4* as a function of the number of cells. They were computed by the checkMesh utility of OpenFOAM®.

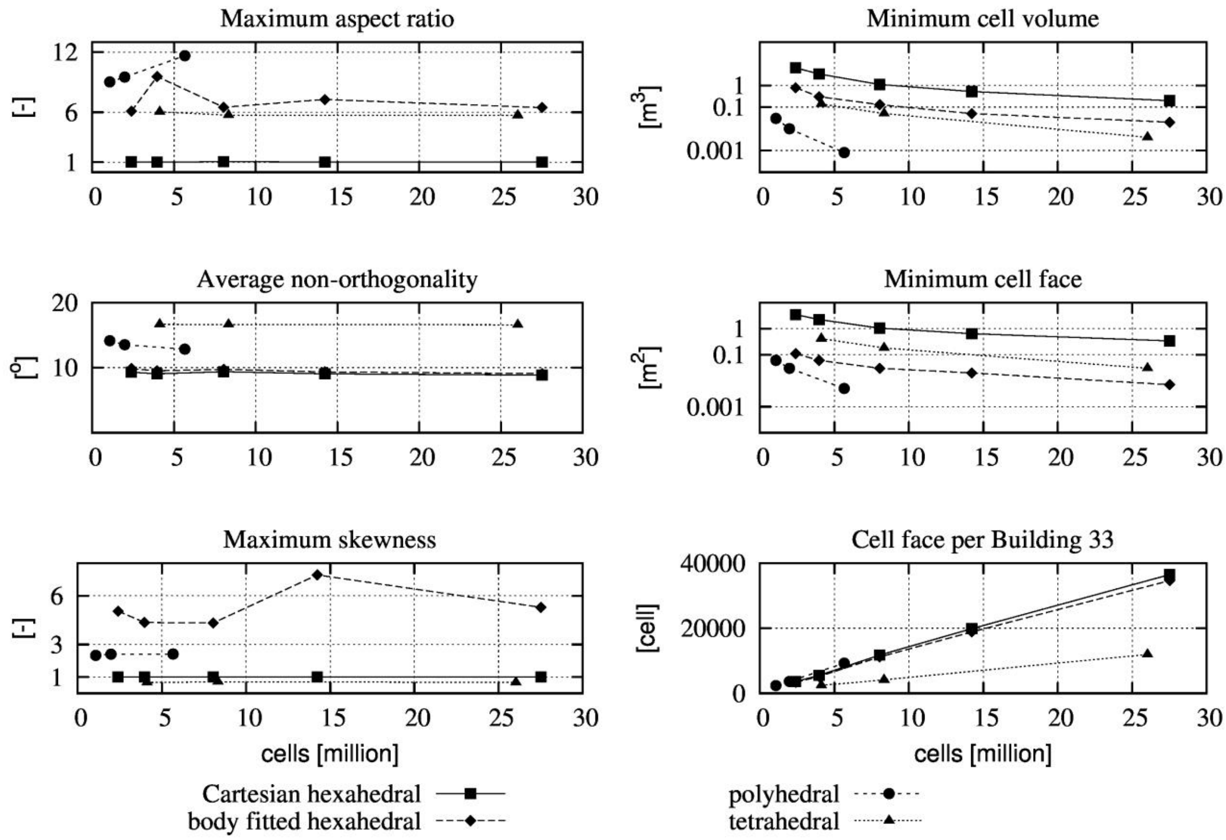

Fig. 4. Mesh quality as a function of cell number, in view of metrics explained in Section 2.3.2.

Maximum aspect ratio is highest for the polyhedral mesh, the tetrahedral and body fitted hexahedral ones are approximately half of it, while the Cartesian hexahedral mesh has an average aspect ratio of 1 as it can be expected.

The non-orthogonality is highest for the tetrahedral meshes, followed by the polyhedral ones, while all hexahedral based meshes have a constant value of 10^o. Although these meshes are mainly Cartesian where 0^o value is expected, by halving the cells this rule is broken for different sized neighbors. In *Fig. 3* it can be observed, how this affects the non-orthogonality. The angle for a transition of this kind in 2D can be computed as the ratio of the edges, $1:3$ as can be seen in *Fig. 3* (angle α). This is an angle of approximately 20^o which is averaged with the rest 0^o values resulting in this 10^o average.

Maximum skewness is the highest for the body fitted hexahedral mesh. For this metric no average value is given by the utility, it shows only the values of the worst quality cells. In that mesh, cells with skewness vector 3 times greater than the face area vector occur.

Minimum cell volume and face area decrease vary rapidly with the increase of resolution. The creation of polyhedral mesh is done by splitting the tetrahedral first, so smaller volumes and face areas occur in case of the polyhedral meshes. This can also be seen in *Fig. 2*.

About the expansion ratio it can be said, that it was set to maximum 1.3 in case of the tetrahedral meshes. For the snappyHexMesh meshes, neighboring cells can differ by a factor of 2 in edge length due to halving cells when refining locally. For unstructured meshes, the cell volume change in neighboring cells is a more useful indicator of the smoothness of transition between smaller and larger cells than expansion ratio. In case of the tetrahedral meshes, the majority of this cell volume change is below 2, while for the polyhedral meshes 6–8% of the neighbors have a cell volume change more than 10. For the hexahedral meshes, the cell volume change is below 2 in 90% of the neighbors and a jump appears around 7–8 due to the refinement method of cell halving which is expected in 3D.

3.2. Convergence

Reaching convergence in complicated geometries and low quality meshes is not always trivial, and in case of this test case, the first computations were often not successful. The best way to reach convergence for all of the cases was explained before. In cases of tetra- and polyhedral meshes, the simulations were unstable also with the described method with default relaxation factors (0.3 for p and 0.7 for the other variables). The cases had to be drastically underrelaxed to reach convergence (0.1 for p and 0.3 for the other variables). In the Best Practice Guideline for ERCOFTAC (European Research Community On Flow, Turbulence and Combustion) special interest group ”Quality and Trust in Industrial CFD” (*ERCOFTAC*, 2000) it is suggested to increase the relaxation factors at the end of the solution to check if the solution holds, thus we checked it for one of the converged underrelaxed simulations. It is important also because *Ferziger* and *Peric* (2002) has shown that the optimum relation between the underrelaxation factors for velocities (uf_u) and pressure (uf_p) is $uf_p = 1 - uf_u$. With raising the relaxation factors each time by 0.1, the combination of 0.2 for *p* and 0.6 for the other variables were reached, but with the default combination the computation crashed again. For this reason, results with the low underrelaxation factors were investigated in the paper.

The difference between the convergence behavior of the hexahedral and polyhedral based meshes is not only their stability. Residual history is smoother for the hexahedral meshes, which makes them a more suitable tool for regulatory purpose simulations, where robustness is a big advantage and can save a lot of time for the operator.

It is an important question what may cause the instability of the tetrahedral and in one case also the polyhedral simulations. Looking at the quality metrics of the meshes, one similar behavior was found for the non-orthogality of the meshes, which can be seen in *Fig. 4*. It is clear that the tetrahedral meshes have the highest non-orthogonality followed by the polyhedral meshes, what can cause the instabilities. This indicates that gradient discretization is also problematic. *Ferziger* and *Peric* (2002) show that in the discretization of non-orthogonal grids of the general transport equation mixed derivatives arise for the diffusive term. They say that if the angle between gridlines is small and aspect ratio is large, the coefficients of these mixed derivatives may be larger than the diagonal coefficients, which can lead to numerical problems. The checkMesh utility of OpenFOAM® reports the number of cells above the non-orthogonality threshold, which is given as 70^o as a default. Although the tetrahedral meshes have higher averages of non-orthogonality, their maximum values never reached this threshold. For the polyhedral ones on the other hand, there were around 10 highly non-orthogonal cells in each mesh.

The convergence behavior of the meshes in general is explained in *Table 3*, where the necessary number of iterations is shown for each mesh, separately for the first order initialization (full upwind-11)/linearUpwind for momentum, first order for turbulence variables (mixed-21)/all higher order (full linearUpwind-22) variations. Convergence is considered when a plateau is reached in the residuals for all variables, see *Fig. 5*. For the meshes where the residuals were not smooth, other variables were also checked to stay stable.

Table 3. Necessary iterations for convergence (full upwind-11/mixed-21/full linearUpwind-22)

	coarsest				**finest**
polyhedral-11	500	–	5000	–	3000
polyhedral-21	+2500	–	+2500	–	+2500
polyhedral-22	+2500	–	+3000	–	+3000
tetrahedral-11	2000	–	2000	–	3000
tetrahedral-21	+1500	–	+1500	–	+2500
tetrahedral-22	+3500	–	+4500	–	+2500
Cartesian hexahedral-11	500	2500	2000	2500	3000
Cartesian hexahedral-21	+1000	+1000	+1000	+1000	+1500
Cartesian hexahedral-22	+500	+2000	+1000	+1000	+1500
body fitted hexahedral-11	1000	1500	1500	2000	2000
body fitted hexahedral-21	+500	+500	+1000	+1000	+1000
body fitted hexahedral-22	+1000	+1000	+1000	+1000	+1000

It can be observed that more iteration is necessary for more cells to reach the first converged state than the expected iterations for linear solvers. The outstanding value of 5000 for the medium polyhedral mesh can be explained by the instability of the computation which made heavy underrelaxation necessary.

In general, the iteration numbers are of the same order of magnitude for all of the meshes. The most orderly results are given by the snapped hexahedral meshes, which underlines again their robustness for operational simulations.

No big difference can be seen between the snapped and Cartesian hexahedral meshes, but in some cases periodic oscillation occurred using a Cartesian mesh. This reduced for the higher order computations, see *Fig. 5*.

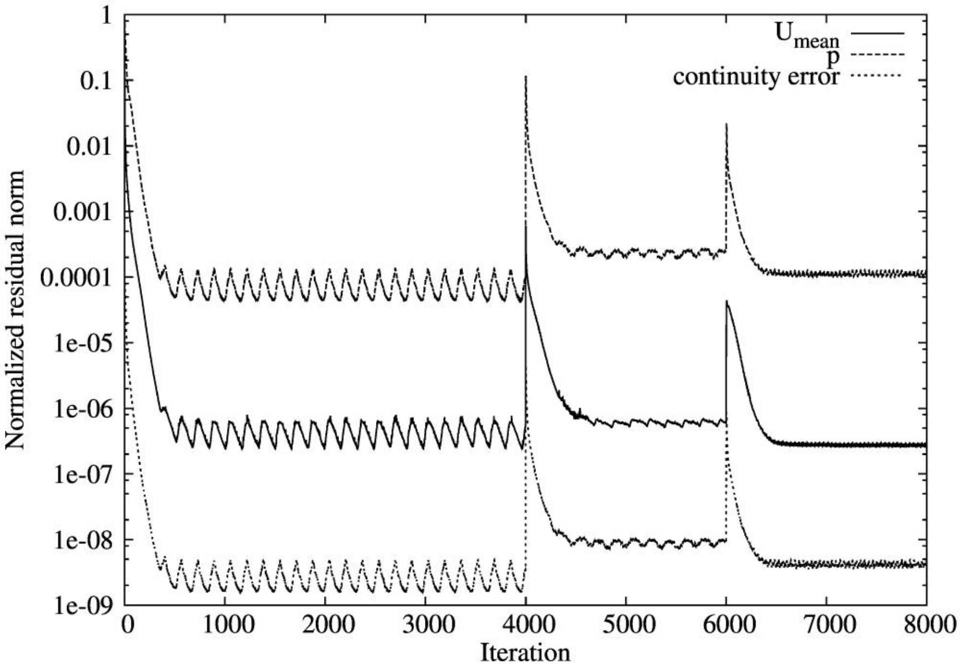

Fig. 5. Residual behavior of a Cartesian mesh.

Turning to the value of the residual norm and its drop from the beginning of the computation we observed, that this case is too complex and values do not reach the machine accuracy in single precision mode. The lowest drop is found in each case for the Poisson equation for the pressure, followed by the lateral and vertical mean velocity components. Another general observation is that all values drop below 10^{-5} for the first order calculations except for the pressure, while for the linearUpwind, only for the momentum equation this drop is usually smaller, followed by a drop below 10^{-5} again for the full linearUpwind computations. The continuity error had a similar behavior, but the first drop was usually below 10^{-8} (see *Fig. 5* for graphical explanation).

This behavior can be explained by the categorization of *Menter* (2012), who states that the classical example of a globally unstable flow is the flow past bluff bodies (like the buildings). Because of this unsteadiness, periodical changes in the residuals are appearing even if the boundary conditions are steady, like in our case.

3.3. Computational cost analysis

One of the main goals of the paper is to compare the models from a regulatory purpose point of view. When carrying out simulations for, e.g., a government, it is usually not possible to wait several days until the simulation is finished on a cluster, and stability is of high importance. For this reason, the computational costs are also evaluated.

The results of this analysis for all of the meshes can be seen in *Fig. 6*. It is apparent, that the memory usage scales linearly for all of the meshes, and the difference in the mesh types can be explained by the relative number of cell faces, i.e., the polyhedral mesh uses more memory for a given number of cells, while the tetrahedral mesh uses less. There is no significant difference between the two kinds of hexahedral meshes, but it is important to note that the solver itself takes no benefit from the fact that one of them is Cartesian.

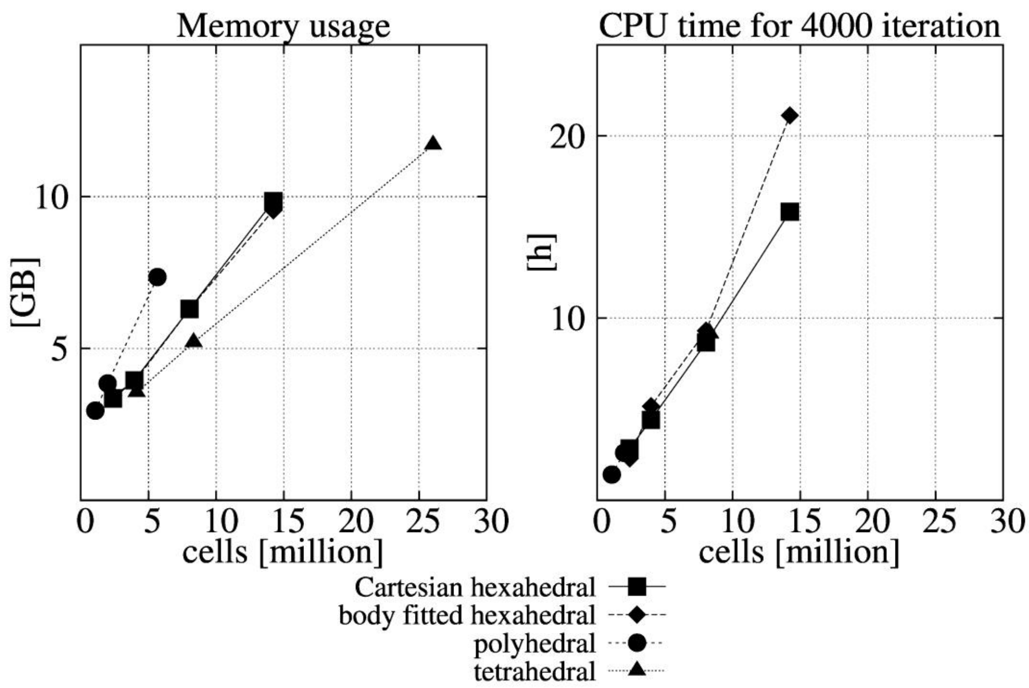

Fig. 6. Computational cost of the simulations for the full upwind simulations, 4000 iterations.

For the comparison of the CPU time, only the relative values are interesting, and it can be seen that the CPU time demand scales linearly with the number of cells, and there is no significant difference in the mesh types. These comparative simulations were carried out on the new cluster of the University of Siegen (http://www.uni-siegen.de/cluster/index.html?lang=en), run for 4000 iterations with first order upwinding for all variables on 24 cores. As a rule of thumb for this setup it can be said, that a simulation result can be obtained in

1 hour/1 million cells. Those meshes which were unstable with the default relaxation factors are omitted from the CPU-time graph.

3.4. Sensitivity to discretization in view of different metrics

Metrics are unavoidable when comparing a lot of different variations, but it is better to check with different metrics to reveal if one of them is biased. The metrics described in Section 2 are used to compare the performance of 4 mesh types, 3–5 spatial resolutions, and 3 discretization scheme combinations for the convective term of the transport equations. Hit rate results for all the cases investigated are shown in *Fig. 7* as a function of the number of cells. The metric based on *L2* normalization can be seen in *Fig. 8* also as a function of the number of cells.

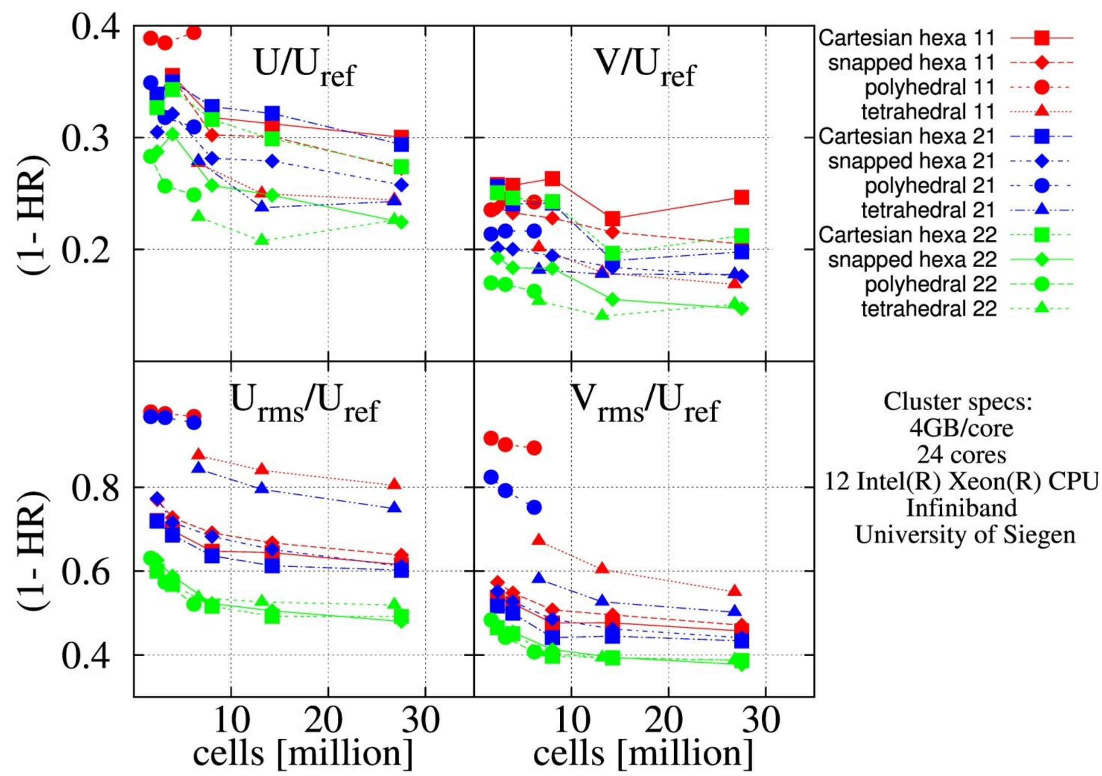

Fig. 7. Sensitivity to discretization, hit rate metric (full upwind-11/mixed-21/full linearUpwind-22).

Comparing the hit rate metric results in *Fig. 7* and the *L2* norm metric results in *Fig. 8* it is important to note, that in case of the hit rates, an ”1 – *HR*” is shown to make them visually similar. Thus, on both figures the smaller is the better. However, the interpretation is very different. In case of the hit rate figure, a smaller value means that more points became ”hits”, the difference between simulation and experiment getting to the acceptable range. Once a point is in this range, the hit rate will not improve even if the results get closer to each other. On the other hand, for the *L2* norm metric, a smaller value means that the difference between simulation and experiment got smaller.

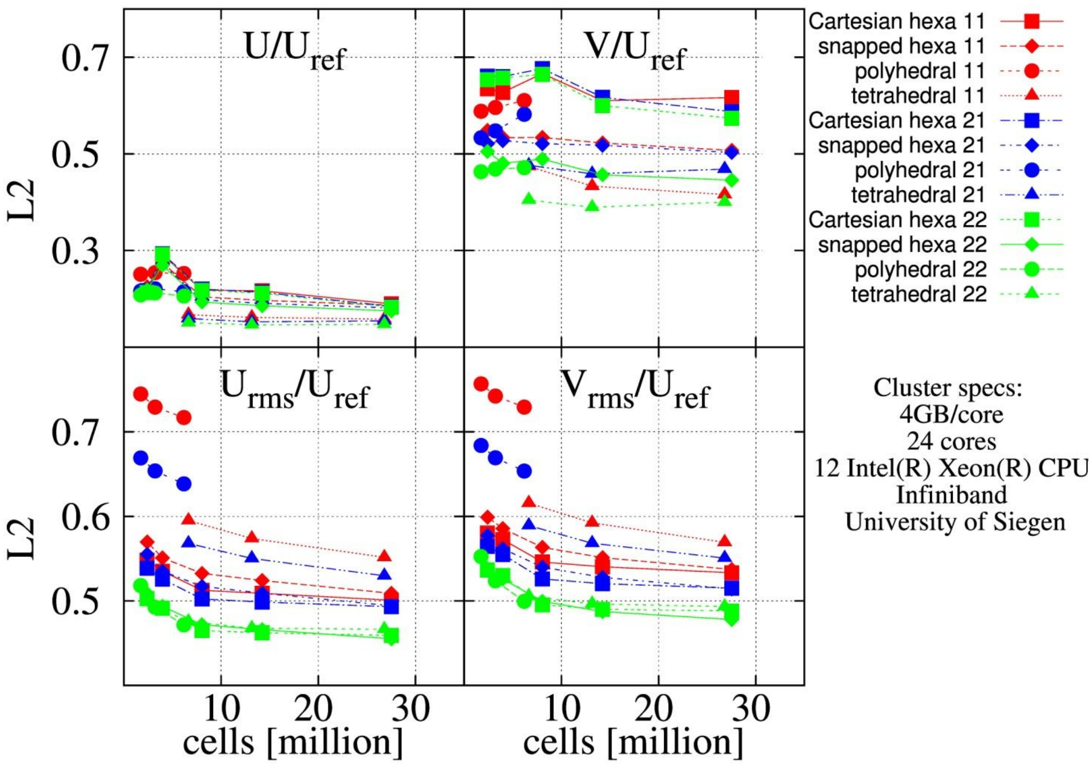

Fig. 8. Sensitivity to discretization, *L2* metric (full upwind-11/mixed-21/full linearUpwind-22).

For the absolute value of the hit rate metric for the mean velocity values it can be said, that these high hit rates are good results for this complex case. Similar values were found by *Efthimiou et al.* (2011) for two other codes, Andrea® and Star-CD®, and by *Franke et al.* (2012b) and *Rakai* and *Franke* (2012) for the ANSYS® Fluent code for the mean velocities. No further exact comments can be made for the turbulent quantities, as the threshold value was chosen arbitrarily and not based on measurement uncertainties. In the VDI guideline (*VDI*, 2005) an acceptable HR value is given for certain test cases, thresholds, and measurement points, but it is not easily transferable to a totally different case.

The absolute value of the *L2* norm metrics can be interpreted as a kind of relative error, showing that for the streamwise velocity results, where the values are essentially higher, the metric is smaller than for all the other variables. For the conclusions drawn later, the absolute value of this metric is not considered.

The conclusions which can be drawn from *Fig. 8* of the *L2* metric norm are the following:

1. For streamwise velocities, tetrahedral meshes perform outstandingly better.

From theoretical point of view, the smallest numerical error is expected from the hexahedral meshes. The reason for this is shown by *Juretic* and *Gosman* (2010): because the hexahedral mesh is aligned with the flow, the errors in fluxes cancel. Explanation for the superior performance of the same mesh size for the tetrahedral meshes in this case can be that those were made with the Delauney algorithm, so they are not “wasting” so many cells in the middle of the domain where there is no geometric feature to disturb the flow, so the gradients are small and do not make high mesh resolution necessary. In case of the hexahedral meshes, the underlying original mesh block has a quite high density. This can be seen in the two coarse meshes compared in *Fig 9*. It is also seen that the transition of tetrahedral cells is smoother from the fine to the coarse cells, and above the canopy where there are still strong gradients, the hexahedral meshes are not resolved enough. See *Fig. 10* for the visualization of these gradients above the urban canopy. A line is shown in *Fig. 9* below which high gradients occur in the solution.

Franke et al. (2012b) used also a block-structured hexahedral mesh for their investigations with ANSYS® Fluent and had better performance also in the mean velocities. That mesh is not automatically generated and has very different mesh quality metrics than the automatic snappyHexMesh meshes (average non-orthogonality 2.64, maximum skewness 1.47, and smooth cell volume transition). The worse results of the automatic hexahedral meshes can be explained by their larger and lower quality cells in the most important regions shown in *Fig. 9*.

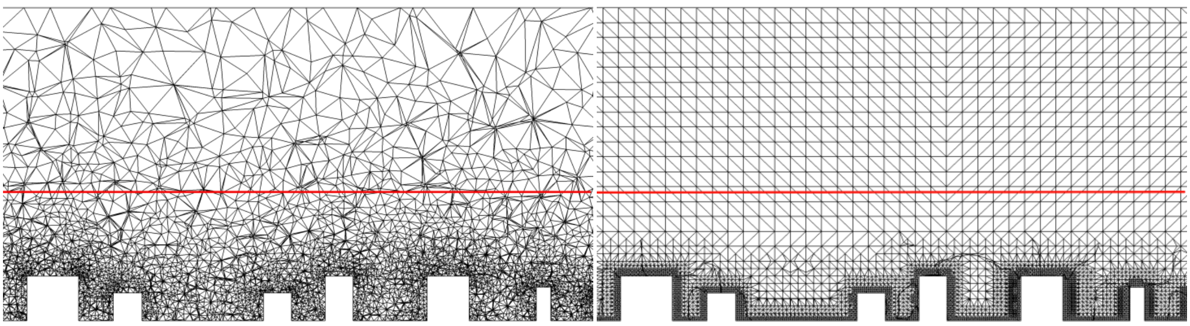

Fig. 9. Tetrahedral (6.65×10^6 cells) and hexahedral (8.0×10^6 cells) mesh cross sections (diagonal lines are just visualization tool specific features in the hexahedral mesh).

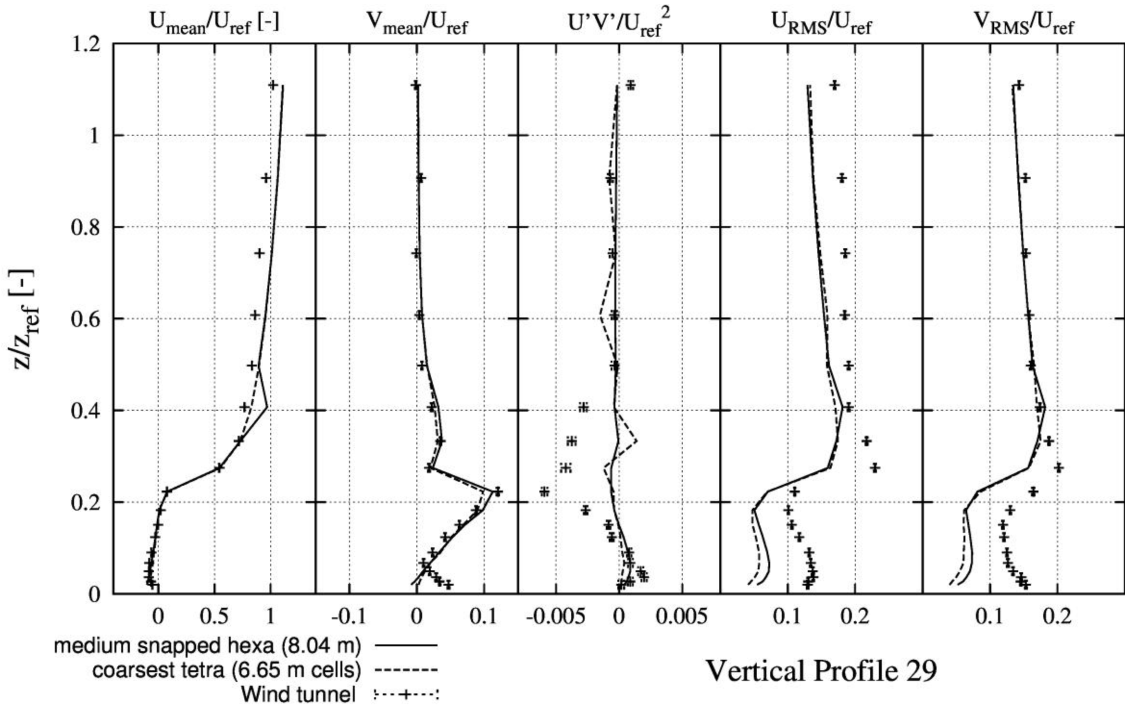

Fig. 10. Profile 29 of one tetrahedral (6.65 $\times 10^6$) and one hexahedral (8.0 $\times 10^6$) mesh (full linearUpwind solution).

2. Better performance of the tetrahedral meshes is not so apparent for lateral velocity, and disappears for the rms values.

To better understand this phenomenon, *Fig. 10* shows the profiles compared at location 29 (see *Fig. 1*) which is in the yard of an 18 m high building. In the non-dimensional scale 0.18 is the top of the building and it can be observed that changes in streamwise mean velocity reach 0.4, while for the other values the maximum is 0.3. So the smoother transition of the tetra mesh can help to better resolve the streamwise velocity, but for the other values it is not so important. The oscillations on the profiles for the tetra meshes can be found on other profiles computed with OpenFOAM® as well. They may be a consequence of the instability of the simulations, however, for the ANSYS® Fluent results they do not appear. This phenomenon needs further investigation.

3. Full second order solutions perform better already for the mean values, but that difference competes with the CPU-time cost of the results. For the turbulent quantities, however, full second order solutions are outstanding.

Theoretically this is obvious as higher order terms are more accurate, but on the other hand, this can amplify the errors in the modeling assumptions. In the Michel-Stadt case the higher order results for the simulation always compare better to the experimental values. It must be kept in mind that not all micrometeorological models use higher order advective terms. As the turbulent quantities are used for the dispersion calculations, it can have a significant effect and higher order terms are suggested.

4. Polyhedral meshes have very low performance compared to all the other cases if not full second order discretization is used.

This can be a result of the larger volumes in those meshes and the large cell volume changes explained, strengthening the numerical errors. It is suggested to use polyhedral meshes only with higher order convective/advective terms, as those metrics are comparable with the other mesh types.

5. The Cartesian hexahedral meshes have lower performance in the mean velocities, but this disappears for the turbulent statistics.

More comparable results for rms value prediction need further investigation. This can be caused by the generally wrong rms predictions for all mesh types and by the numerical errors canceling the modeling errors.

6. There is a jump of low performance for the second coarsest hexahedral meshes which is visible both in the hit rate metric and *L2* norm metric.

This is a sign that mesh refinement does not always lead to improved solutions because of the error cancellation explained above. Also the importance of investigation of mesh dependency on more meshes must be noted.

4. Conclusions and outlook

Sensitivity of four different metrics to compare experimental and simulation results was investigated for a test case of an idealized Central European city center, Michel-Stadt. The numerical discretization approaches were compared with four different mesh types, at least 3 resolutions for each of them, and different discretization procedures of the convective/advective term in a numerical experiment.

It was found that snappyHexMesh meshes are more stable computationally. so they are more appropriate for operational purposes, although their metric performance is not as good as that of the tetrahedral meshes. The lower validation metric performance is not true in general for all hexahedral meshes, more time consuming block-structured meshes with higher mesh quality metrics can be generated which are both stable and more accurate.

For diagonal components of the Reynolds stresses, i.e., the rms values in experimental results, discretization schemes of the convective terms have a striking but expectable effect which must be kept in mind for dispersion studies where their value effects turbulent diffusion. Numerical discretization differences can cause almost 20 % change in the hit rate metric.

There are still many open questions to be further investigated, e.g., the oscillation in the tetrahedral profiles, correspondence between stability and mesh quality of the different mesh types, and the generation of the polyhedral mesh to explain their low upwind validation metrics. This will be carried out through further more detailed analyses of the datasets.

The work with Michel-Stadt continues in the framework of COST Action ES 1006 with numerical uncertainty estimation and dispersion studies for continuous and puff passive scalar sources. The Action involves several research groups who use different codes, including prognostic microscale obstacle resolving meteorological models, diagnostic flow models, and operational Gaussian type plume models. After investigations of the setup shown in this paper, a blind test will be carried out to evaluate the use of local-scale emergency prediction and response tools for airborne hazards in built environments.

Acknowledgement–This research was financed by a scholarship of the Hungarian Government and the project Talent Care and Cultivation in the Scientific Workshops of BME. The project is supported by the grant TAMOP-4.2.2/B-10/1-2010-0009. It is also related to the scientific programme of the project Development of Quality-Oriented and Harmonized R+D+I Strategy and the Functional Model at BME, the New Hungary Development Plan (Project ID: TAMOP-4.2.1/B-09/1/KMR-2010-0002), and the K 108936 ID project of the Hungarian Scientific Research Fund. Collaboration of the authors was possible thanks to two DAAD (German Academic Exchange Service) research grants, number A/10/82525 and A/11/83345.

References

Ansys®, 2009: Ansys Fluent 14.0 Theory Guide. Canonsburg, Pennsylvania.

Baklanov, A. and *Nuterman, R.B.,* 2009: Multi-scale atmospheric environment modelling for urban areas. *Adv. Sci. Res. 3,* 53–57.

Baklanov, A., 2000: Application of CFD methods for modelling in air pollution problems: possibilities and gaps. *Environ. Monit. Assess. 65,* 181–189.

Balczó, M., Balogh, M., Goricsan, I., Nagel, T., Suda, J., and *Lajos, T.,* 2011: Air quality around motorway tunnels in complex terrain – computational fluid dynamics modeling and comparison to wind tunnel data. *Időjárás 115,* 179–204.

Balogh, M., Parente, A., and *Benocci, C.,* 2012: RANS simulation of ABL flow over complex terrains applying an Enhanced k-ε model and wall function formulation: Implementation and comparison for fluent and OpenFOAM®. *J. Wind Eng. Ind. Aerod. 104–106,* 360–368.

Blocken, B., Stathopoulos, T., and *Carmeliet, J.,* 2007a: CFD evaluation of wind speed conditions in passages between parallel buildings – effect of wall-function roughness modifications for the atmospheric boundary layer flow. *J. Wind Eng. Ind. Aerod. 95,* 941–962.

Blocken, B., Stathopoulos, T., and *Carmeliet, J.,* 2007b: CFD simulation of the atmospheric boundary layer: wall function problems. *Atmos. Environ. 41,* 238–252.

Britter, R.E. and *Hanna, S.R.,* 2003: Flow and dispersion in urban areas. *Annu. Rev. Fluid Mech. 35,* 469–96.

COST ES1006, 2012: COST ES1006 Background and Justification Document. *COST. Action ES 1006: Evaluation, improvement and guidance for the use of local-scale emergency prediction and response tools for airborne hazards in built environments.*

Durbin, P.A., 1996: On the k- ε stagnation point anomaly. *Int. J. Heat Fluid Flow 17,* 89–90.

Eca, L. and *Hoekstra, M.*, 2008: Testing Uncertainty Estimation and Validation Procedures in the Flow Around a Backward Facing Step. In *Proceedings of the 3rd Workshop on CFD Uncertainty Analysis.*

Efthimiou, G.C., Hertwig, D., Fischer, R., Harms, F., Bastigkeit, I., Koutsourakis, N., Theodoridis, A., Bartzis, J.G., and *Leitl, B.*, 2011: Wind flow validation for individual exposure studies. In *Proceedings of the 13th International Conference on Wind Engineering (ICWE13),* Amsterdam, The Netherlands.

Ehrhard, J., Kunz, R., and *Moussiopoulos, N.,* 2000: On the performance and applicability of nonlinear two equation turbulence models for urban air quality modelling. *Environ. Monit. Assess. 65,* 201–209.

Eichhorn, Dr. J., 2008: MISKAM manual for version 5. Spielplatz 2 55263 Wackernheim.

ERCOFTAC, 2000: Best Practice Guidelines. *ERCOFTAC Special Interest Group on"Quality and Trust in Industrial CFD".*

Ferziger, J.H. and *Peric, M.,* 2002: Computational Methods for Fluid Dynamics. Springer, Berlin Heidelberg New-York

Fischer, R., Bastigkeit, I., Leitl, B., and *Schatzmann, M.,* 2010: Generation of spatio-temporally high resolved datasets for the validation of LES- models simulating flow and dispersion phenomena within the lower atmospheric boundary layer. In *Proceedings of The Fifth International Symposium on Computational Wind Engineering (CWE2010),* Chapel Hill, North Carolina, USA.

Franke, J., Hellsten, A., Schlünzen, H., and *Carissimo, B.,* 2007: Best Practice Guideline for the CFD Simulation of Flows in the Urban Environment. *COST Action 732: Quality Assurance and Improvement of Microscale Meteorological Models.*

Franke, J., 2010: A review of verification and validation in relation to CWE. In *Proceedings of the Fifth International Symposium on Computational Wind Engineering (CWE2010)* Chapel Hill, North Carolina, USA, May 23–27, 2010.

Franke, J., Hellsten, A., Schlunzen, K.H., and Carissimo, B. 2011. 2011 The COST 732 Best Practice Guideline for CFD simulation of flows in the urban environment: a summary. *International Journal of Environment and Pollution, 44(1–4), 419–427.*

Franke, J., Sturm, M., and *Kalmbach, C.,* 2012a: Validation of OpenFOAM® 1.6.x with the German VDI guideline for obstacle resolving microscale models. *J. Wind Eng. Ind. Aerod. 104–106,* 350–359.

Franke, J., Laaser, A., Bieker, B., and *Kempfer, T.* 2012b: Sensitivity analysis of RANS simulations for flow and dispersion in the generic European City Centre Michel-Stadt. In *Proceedings of Conference on Modelling Fluid Flow.* Budapest, Hungary, Sept 4–7 2012.

Hefny, M.M. and *Ooka, R.,* 2009: CFD analysis of pollutant dispersion around buildings: Effect of cell geometry. *J. Build. Environ. 44,* 1699–1706.

Janssen, W.D, Blocken, B., and *van Hoof, T.* 2012: Pedestrian wind comfort around buildings: comparison of wind comfort criteria based on whole-flow field data for a complex case study. *J. Build. Environ. accepted for publication.*

Jasak, H., 1996: Error Analysis and Estimation for the Finite Volume Method with Application to Fluid Flows. *PhD. Thesis, Imperial College of Science, Technology and Medicine*.

Juretic, F. and *Gosman, A.D.*, 2010: Error Analysis of the Finite-Volume Method with respect to Mesh Type. *Num. Heat Transfer 57*, 414–439.

Leelőssy, Á., 2012: Baleseti kibocsátásból származó szennyezőanyagok lokális skálájú terjedésének modellezése. *M.Sc. thesis, Eötvös Lóránd Univ. Dep. Meteorology*. (In Hungarian)

Lun, Y.F., Mochida, A., Murakami, S., Yoshino, H., and *Shirasawa, T.,* 2003: Numerical simulation of flow over topographic features by revised $k-\varepsilon$ models. *J. Wind Eng. Ind. Aerod. 91,* 231–245.

Menter, F.R., 2012: Best Practice: Scale-Resolving Simulations in ANSYS® *CFD. ANSYS®,* Germany.

Mészáros, R., Vincze, Cs., and *Lagzi, I.,* 2010: Simulation of accidental release using a coupled transport (TREX) and numerical weather prediction (ALADIN) model. *Időjárás 114,* 101–120.

Oberkampf, W.L., and *Trucano, T.G.,* 2002: Verification and validation in computational fluid dynamics. *Prog. Aerospace Sci, 38.* 209–272.

OpenCFD Limited, 2011: OpenFOAM® User Guide – Version 2.0.0. OpenCFD Limited.

O'Sullivan, J.P., Archer, R.A., and *Flay, G.J.,* 2011: Consistent boundary conditions for flows within the atmospheric boundary layer. *J. Wind Eng. Ind. Aerod. 99,* 65–77.

Parente, A., Gorlé, C., van Beeck, J., and *Benocci, C.* 2010: A Comprehensive Modelling Approach for the Neutral Atmospheric Boundary Layer: Consistent Inflow Conditions, Wall Function and Turbulence Model. *Bound-Lay. Meteorol. 140,* 411–428.

Rakai, A. and *Franke, J.,* 2012: Validation of two RANS solvers with flow data of the flat roof Michel-Stadt case. In *Proc. 8th International Conference on Air Quality – Science and Application,* Athens, Greece.

Rakai, A., and *Kristóf, G.,* 2010: CFD Simulation of Flow over a Mock Urban Setting Using OpenFOAM®. In Gépészet 2010: *Proceedings of the Seventh Conference on Mechanical Engineering.* Budapest, Hungary.

Richards, P.J. and *Hoxey, R.,* 1993: Appropriate boundary conditions for computational wind engineering models using the k − turbulence model. *J. Wind Eng. Ind. Aerod. 47,* 145–153.

Roache, P.J., 1997: Quantification of Uncertainty in Computational Fluid Dynamics. *Annu. Rev. Fluid Mech. 29,* 123–60.

Schatzmann, M., Olesen, H., and *Franke, J.* 2009: COST 732 Model Evaluation Case Studies: Approach and Results. *COST Action 732: Quality Assurance and Improvement of Microscale Meteorological Models.*

S*chatzmann, M.* and *Leitl, B.,* 2011: Issues with validation of urban flow and dispersion CFD models. *J. Wind Eng. Ind. Aerod. 99,* 169–186.

Stull, R.B., 1988: An Introduction to Boundary Layer Meteorology. Kluwer Academic Pub.

Tominaga, Y., Mochida, A., Yoshie, R., Kataoka, H., Nozu, T,, Kazuyoshi, Y,, M., and *Shirasawa, T.,* 2008: AIJ guidelines for practical applications of CFD to pedestrian wind environment around buildings . *J. Wind Eng. Ind. Aerod. 96,* 1749–1761.

T*ominaga, Y., Mochida, A., Shirasawa, T., Yoshie, R., Kataoka, H., Harimoto, K., and Nozu, T.,* 2004: Cross Comparison of CFD Results of Wind Environment at Pedestrian Level around a High-rise Building and within a Building Complex. *J. Asian Arch. Build. Engin., 3.*

VDI., 2005: Environmental Meteorology – Prognostic microscale wind field models – Evaluation for flow around buildings and obstacles, *VDI guideline 3783, Part 9.*

Wright, N.G., and *Easom, G.J.,* 2003: Non-linear k − turbulence model results for flow over a building at full scale. *Appl. Math. model. 27,* 1013–1033.

Yang, Y., Gu, M., Chen, S., and *Jin, X.,* 2007: New inflow boundary conditions for modeling the neutral equilibrium atmospheric boundary layer in computational wind engineering. *J. Wind Eng. Ind. Aerod. 97,* 88–95.

Yoshie, R., Mochida, A., Tominaga, Y., Kataoka, H., and *Yoshikawa, M.,* 2005: Cross Comparison of CFD Prediction for Wind Environment at Pedestrian Level around Buildings Part 1-2. In *Proceedings of the 6th Asia-Pacific Conference on Wind Engineering (APCWE-VI).*Seoul, Korea, September 12–14, 2005.